First-Principles Study of Bond Rupture of Entangled Polymer Chains

A. Marco Saitta* and Michael L. Klein

Center for Molecular Modeling, Department of Chemistry, University of Pennsylvania, Philadelphia, Pennsylvania 19104-6323

Received: December 7, 1999; In Final Form: January 20, 2000

The entanglement of neighboring chains is a common topological defect found in polymers. The limiting stress and mechanism of rupture of two entangled polyethylene chains, subjected to external loading, has been investigated using first-principles molecular dynamics calculations. Our results show that intermolecular entanglement significantly weakens each polymer strand. Interchain bond−bond or atom−bond friction is the major driving force in the rupture process.

I. Introduction

The physical properties of polymer films are significantly affected by defects that reduce their crystallinity. Topological defects, such as chain entanglements, play an important role since they are unavoidably generated during crystallization. The dynamics of dense polymeric systems are known to be dominated by entanglements,[1] which give rise to a network of constraints that reduce the mobility of each molecule. Such defects are characterized either by single-molecule simple knots,[2] or by multichain structures,[3] which range from simple entanglements to composite knots. The simplest single-chain knots are consistently observed in real polymers,[4] including DNA,[5] and are widely studied with computer simulations.[6] Tensile strength, resistance, and many other mechanical properties of polymeric systems dramatically change in the presence of entanglements,[7] and efforts have been made to establish how ultimate tensile stress is related to their density and morphology.[3]

In this Letter, we examine the behavior and stability of two entangled polymer molecules subject to tensile stress. In analogy with our recent study of a self-entangled (knotted) strand,[8,9] we study the behavior of two entangled long-chain *n*-alkanes using first-principles molecular dynamics (MD) calculations. Anticipating our results we find that for the configurations shown in Figure 1 the strain energy per bond at rupture is about 90% of the value for a linear molecule. In this sense, the presence of the entanglement weakens the single-chain resistance to tension. However, entanglement necessarily involves a second chain, which stores half of the total strain energy. The net result is that entanglements increase the resistance of macroscopic semicrystalline polymer films to crazing and fracture.[7]

II. Computational Details

The first-principles calculations were carried out with a supercell technique using Car−Parrinello[10] molecular dynamics (CPMD),[11] based on density-functional theory with Becke and Lee−Yang−Parr (BLYP)[12] for the exchange and correlation functionals. CPMD is known to handle systems containing up to a few hundred atoms for picosecond time scales. This limitation prevents the full atomic-scale study of entanglement in polymer blends but, as will be pointed out later, we model the problem with systems large enough for a proper description of the relevant processes at the chemical bond level, and still within the computational reach of the method. A valence electron pseudopotential/plane-wave scheme was employed, with a kinetic-energy cutoff of 60 Ry and a Γ-point sampling of the Brillouin zone. Since chain rupture yields unpaired electrons, the spin variables were handled through the so-called local spin-density approximation.[13] As shown elsewhere,[8,9] this ab initio framework provides results on the structural properties and bond energetics accurate to within 1% and 2%, respectively. To follow the dynamical evolution of the system at room temperature ($T = 300$ K), we employed a time step of 6.0 a.u. (= 0.145 *fs*). The starting configurations in the CPMD calculations were obtained from a series of classical MD simulations[14] on a united atom (UA) model,[15] in which methylene ($-CH_2-$) or methyl ($-CH_3$) groups are considered as "pseudoatoms" interacting via an empirical force field. The model included harmonic bond-stretching, harmonic bond-bending, a torsional potential, and a Lennard−Jones (LJ) interaction between nonbonded atoms.[16]

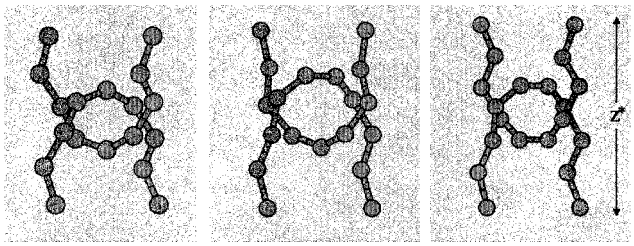

Figure 1. Snapshots of the carbon backbones of two entangled alkanes as obtained from the classical MD simulations. These structures were used as the initial configurations in the CPMD calculations: bond−bond (right panel), bond−atom (middle panel), and atom−atom (left panel) friction cases.

The initial system for the classical simulation consisted of two straight *n*-alkane molecules (that we label as "*A*" and "*B*") perpendicular to each other in a cross-like configuration. We refer to the original directions of the axes of the two alkanes as *x* and *y*, respectively. The *z* coordinates of the two pseudoatoms at the end of each chain are constrained during the simulations to fixed values z_A and z_B, respectively. We examined three different cases: (i) bond−bond friction, likely the most common case, where the crosspoint corresponds to the midpoint of a C−C bond for both molecules; (ii) bond−atom friction, where one

* Author to whom correspondence should be addressed. E-mail: saitta@cmm.chem.upenn.edu.

10.1021/jp994299n CCC: $19.00
Published on Web 02/23/2000

of the two alkanes has a C atom at the midpoint; (iii) atom−atom friction. The three situations are mimicked using a decane−decane ($C_{10}H_{22}$), a decane−nonane (C_9H_{20}), and a nonane−nonane systems, respectively. Chain length effects were checked for the more interesting "bond−bond" case using a dodecane−dodecane ($C_{12}H_{26}$) system and a tetradecane−tetradecane ($C_{14}H_{30}$) system, which did not display any different qualitative or quantitative behavior.

The difference $z^* = z_A - z_B$ is the system "reaction" coordinate on which we act on to apply tensile stress to the system to generate the chain entanglement. In the present case, stretching is not applied along the direction of the chain end-to-end vector, as it was in our previous study of the linear and knotted single strands, but perpendicularly to it. In the initial configuration described above we start with $z^* = -\sigma$, where σ is the LJ parameter for the chains. The procedure we follow consists of successively increasing the amount of the separation z^*, from this negative value to larger and larger positive values. The molecules are thus forced to bend to comply with the strong repulsive short-range LJ potential. The U-shaped bent chains thus generated lie approximately in the *xz* and the *yz* planes, for molecules *A* and *B* respectively, and they are mutually orthogonal. For each value of z^* the system was first evolved using classical MD for about 200 ps, and then cooled with a simulated annealing technique for about 50 ps, to find the constrained structural energy minimum. The classical strain energy per bond was monitored at the end of each set of simulations (i.e., at the ground state corresponding to each z^*). Experience from analogous analysis for straight and knotted alkanes[9] tells us that the order of magnitude of classical strain energy per bond should be above 20 kcal/mol, to eventually cause bond rupture within the typical picosecond time window of first-principles MD simulations.

Under loads close to the relevant strain energy, the shape of the system is totally dominated by the short-range repulsion between the central portions of the molecules, where the curvature is significantly larger than it is at the ends of the chains. In Figure 1 we report snapshots of typical configurations for the three cases we focused on. The shape of the system under stress closely resembles two interpenetrating half-rings. Thus, the system studied can also be regarded as a unit segment of a catenane, which is a molecular superstructure consisting of closed interpenetrating loops.[17,18]

III. Results and Discussion

The constrained ground-state configurations obtained for each z^* from the classical MD simulations were used as initial sets of coordinates for the quantum mechanical CP calculations. In Figure 2 we report, for the three cases under study, the classical strain energy distributions as obtained at the respective values of z^* that yield a rupture in the first-principles simulations. It is interesting to note that the stress tends to accumulate in the central bonds, which are more subject to the effects of friction. This occurs despite the fact that the classical model strongly favors uniform deformations along the chains. In contrast, as shown in refs,[8,9] straight alkanes under loading tend to store most of their strain energy in the extremal bonds, in the proximity of the constraints. However, as in the present case, friction seems to play a major role for a knotted strand.

The relative importance of the different contributions to total strain is very dependent on the system under examination. In the case of "pure" stretching of a linear alkane along its axis, C−C bond-length deformations can be larger than 20% of the equilibrium values, C−C−C angles are always smaller than

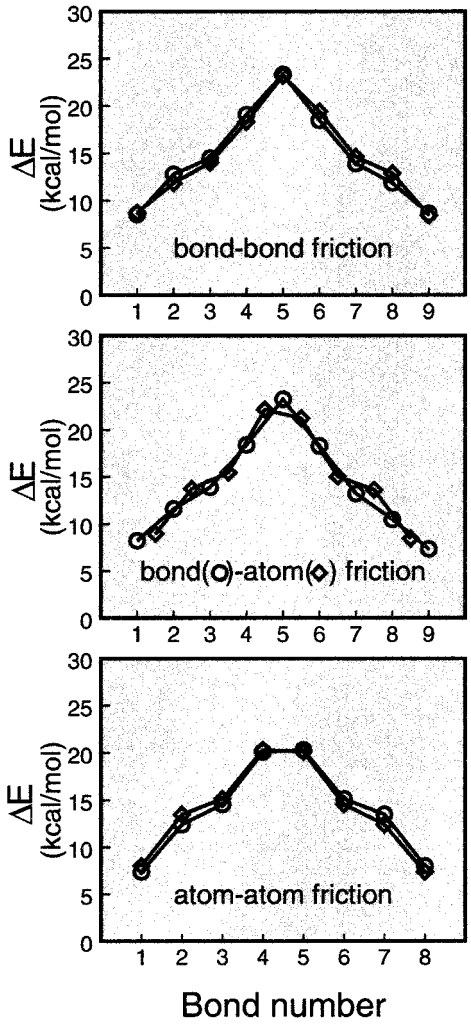

Figure 2. Classical strain energy distributions along the chains at the break separation (see text), for the decane−decane (upper panel), decane−nonane (middle panel), and nonane−nonane (lower panel) systems. The bond numbering of the nonane molecule in the middle panel is shifted by a half unit to be symmetric with respect to the crosspoint.

135°, and torsional strain is negligible. In a knotted chain, where stress is a mixture of stretching and friction contributions, bond-length distortions are up to 15%, while bond-angle bending can exceed 145° along the molecule, and torsions are relevant. In the present case, where friction should be even more important, bond-length elongations are smaller than 12%, bond-angle bending and torsions accounting for most of the strain sustained by the system.

For the three cases we are presently focusing on, room-temperature CPMD simulations were performed for about 1 ps.[19] If chain rupture did not occur, z^* was slightly increased and a new CP simulation carried out. In Figure 3 we display snapshots of the system at the break. In case (i), rupture occurs randomly at the central bond of one of the decane molecules; in case (ii), i.e., bond−atom friction, the chain breaks at the central bond of the $C_{10}H_{22}$ chain; in case (iii), rupture occurs randomly at one of the four bonds adjoining the two central C atoms. The strain energy per bond at rupture is 14.6 kcal/mol, i.e., about 90% of the estimate for a stretched single *n*-alkane.

To assess the importance of possible fixed-strain effects and to estimate the actual force applied to the systems at the break, we employed the same "cantilever" technique successfully adopted in recent classical MD simulations of biomolecules

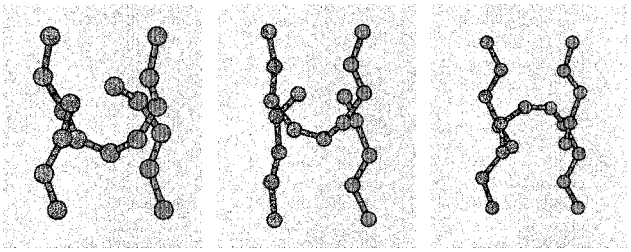

Figure 3. Snapshots of the carbon skeletons at the break for the bond−bond (right panel), bond−atom (middle panel), and atom−atom (left panel) friction cases. Rupture invariably occurs at the bond corresponding to the crosspoint.

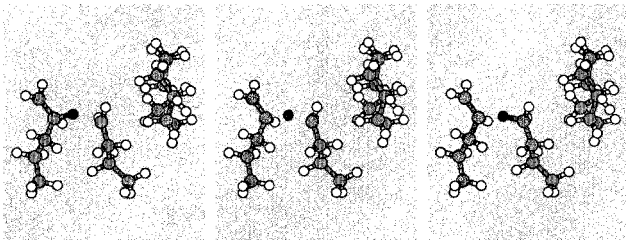

Figure 4. Snapshots of the disproportionation reaction that follows bond rupture. Carbon atoms are shown in gray, hydrogen atoms are displayed in white, and the abstracted hydrogen atom is shown in black. The coplanarity of the α and β carbons at the end of the pentyl radical with their bonded hydrogens (on the left) is a signal of sp^2 hybridization and, thus, of a double bond.

under load.[20] In the present case we attached harmonic springs to the terminal methyl groups. These quasi-static springs act during the simulations to increase the separation z^*. As pointed out in ref 20, we are then able to estimate the force acting on the chains simply by monitoring the elongation of the springs. The forces we measure at the rupture are of the order of 4−5 nN.[21] The energy barriers of the strain-induced dissociation are about 350 kcal/mol. Analogous calculations performed with longer alkanes both containing an even number of carbon atoms (bond−bond friction case) gave similar results, i.e., a broad classical strain energy distribution peaked at the central bond (see Figure 2), which will eventually undergo rupture in the subsequent quantum-mechanical simulations.

In addition to studying the rupture process of entangled chains, the dynamical evolution of the chain fragments was followed. The supercells we use are large enough to avoid interactions with the periodic images before the break occurs, because the entanglement constrains the chains in half-ring conformations. Once the constraint is released at the dissociation, intercell radical interaction is possible, since the net length of the chain fragments is comparable with the *a* and *b* sides of the orthorhombic cell we employed. In cases (i) and (ii), where the chain fragments are both *n*-pentyl radicals, a simple intercell recombination occurs. In case (iii), where *n*-butyl and *n*-pentyl radicals are generated, a different reaction occurs: the unsaturated carbon atom at the end of the C_4H_9• fragment abstracts a hydrogen atom from the β carbon atom of the C_5H_{11}• radical. This atom forms a double bond with the α carbon of the pentyl fragment, thus stabilizing the second unpaired electron (see Figure 4). This reaction, known as disproportionation, is energetically less favorable than recombination. The difference in energy gain we estimate is ca. 23 kcal/mol, in quantitative agreement with experiments.[25] However, both reactions have an activation barrier that is zero within experimental error; thus, the respective constant rates are very similar. In the present case, disproportionation is likely to be favored by steric effects due to the boundary conditions imposed by our simulations. These observations are a signal of the strong chemical reactivity of the alkyl fragments.[26]

IV. Conclusions

In conclusion, the rupture of entangled polymer strands is a bond friction-driven phenomenon, in which entanglement reduces the tensile strength of the individual chains. Recently, related studies[8] have shown that the properties of an overhand "trefoil" knot in a polyethylene chain, subjected to tensile loading, closely follow the well-known behavior of macroscopic ropes.[27] Indeed, these ab initio calculations confirm our common experience that the presence of the knot significantly reduces the tensile strain that can be stored in the strand before breaking. Moreover, the break point in a microscopic polymer strand occurs at either the entrance or exit point of the knot, exactly as in a macroscopic rope.[8,27] Very similar results were recently found in experiments in which actin or DNA filaments were tied in a trefoil knot by means of optical tweezers.[28] Our present results show that, in analogy with the case of knotted molecules,[8] entangled polymers subject to tensile loading behave at an atomistic level exactly as macroscopic ropes, thereby suggesting that stress-induced rupture of unidimensional systems (ropes or polymers) follow universal, size-independent rules. As a byproduct, we observe an example of ultrafast reaction of the chain radical fragments after the break, very similar to findings we discuss elsewhere.[26]

Acknowledgment. We thank E. Wasserman and P. D. Soper for communicating their results prior to publications. This research was supported by Grant NSF CHE9523017 and facilities provided by NSF DMR 9632588.

References and Notes

(1) de Gennes, P.-G. *J. Chem. Phys.* **1971**, *55*, 572; Schleger, P.; Farago, B.; Lartigue, C.; Kollmar, A.; Richter, D. *Phys. Rev. Lett.* **1998**, *81*, 124; Kremer, K.; Grest, G. S.; Carmesin, I. *Phys. Rev. Lett.* **1988**, *61*, 566; Smith, S. W.; Hall, C. K.; Freeman, B. D. *J. Chem. Phys.* **1996**, *104*, 5616.

(2) Atiyha, M. F. *The Geometry and Physics of Knots*; Cambridge University Press: Cambridge, 1990.

(3) Bayer, R. K. *Colloid Polym. Sci.* **1994**, *272*, 910; Bayer, R. K.; Baltá Calleja, F. J.; Kilian, H. G. *Colloid Polym. Sci.* **1997**, *275*, 432.

(4) Frisch, H. L.; Wasserman, E. *J. Am. Chem. Soc.* **1961**, *83*, 3789; Walba, D. M. *Tetrahedron* **1985**, *41*, 3161; Frank-Kamenetskii, M. D.; Lukashin, A. V.; Vologodskii, A. V. *Nature* **1975**, *258*, 398; Frisch, H. L. *New J. Chem.* **1993**, *17*, 697.

(5) Wasserman, S. A.; Cozzarelli, N. R. *Science* **1986**, *232*, 951; Shaw, S. Y.; Wang, J. C. *Science* **1993**, *260*, 533; Sogo, J. M.; Stasiak, A.; Martinez-Robles, M. L.; Krimer, D. B.; Hernandez, P.; Schvartzman, J. B. *J. Mol. Biol.* **1999**, *286*, 637.

(6) Schlick, T.; Olson, W. K. *Science* **1992**, *257*, 1110; Katritch, V.; et al. *Nature* **1996**, *384*, 142; *Nature* **1997**, *388*, 148; Iwata, K.; Tanaka, J. *J. Phys. Chem.* **1992**, *96*, 4100.

(7) Plummer, C. J. G.; Kausch, H.-H. *J. Macromol. Sci.-Phys. B* **1996**, *35*, 637; Crist, B. *Annu. Rev. Mater. Sci.* **1995**, *25*, 295.

(8) Saitta, A. M.; Soper, P. D.; Wasserman, E.; Klein, M. L. *Nature* **1999**, *399*, 46.

(9) Saitta, A. M.; Klein, M. L. *J. Chem. Phys.* **1999**, *111*, 9434.

(10) Car, R.; Parrinello, M. *Phys. Rev. Lett.* **1985**, *55*, 2471.

(11) *CPMD*, version 3.0. Hutter, J.; Ballone, P.; Bernasconi, M.; Focher, P.; Fois, E.; Gödecker, S.; Parrinello, M.; Tuckerman, M. E. MPI für Festkörperforschung and IBM Research Laboratory, Stuttgart and Zürich, 1990−1996.

(12) Becke, A. D. *Phys. Rev. A* **1988**, *38*, 3098; Lee, C.; Yang, W.; Parr, R. G. *Phys. Rev. B* **1988**, *37*, 785.

(13) Perdew, J. P.; Wang, Y. *Phys. Rev. B* **1992**, *45*, 13244.

(14) Martyna, G. J.; et al. PINY Code; *Comput. Phys. Commun.*, in press.

(15) Siepmann, J. I.; Karaborni, S.; Smit, B. *Nature* **1993**, *365*, 330.

(16) Mundy, C. J.; Balasubramanian, S.; Bagchi, K.; Siepmann, J. I.; Klein, M. L. *Faraday Discuss.* **1996**, *104*, 17.

(17) Schill, G. *Catenanes, Rotaxanes, and Knots*; Academic: New York, 1971.

(18) Fujita, M.; Fujita, N.; Ogura, K.; Yamaguchi, K. *Nature* **1999**, *400*, 52.

(19) A rough estimate of the time necessary for the slowest longitudinal phonon to travel along each chain is ∼70 fs.

(20) Grubmüller, H.; Heymann, B.; Tavan, P. *Science* **1996**, *271*, 997; Rief, M.; Oesterhelt, F.; Heymann, B.; Gaub, H. E. *Science* **1997**, *275*, 1295.

(21) Stretching forces in the nN range are likely to be soon attainable in experiments with optical tweezers[22] or atomic force microscope (AFM)[23] techniques. As pointed out in ref 24, the typical loading rate of MD simulations ($\sim 10^{12}$ pN/s) is, however, well beyond the reach of experiments, around 1−10 pN/s for the laser tweezers, and 10^4-10^5 pN/s for AFM.

(22) Cluzel, P.; et al. *Science* **1996**, *271*, 792; Smith, S. B.; Cui, Y. J.; Bustamante, C. *Science* **1996**, *271*, 795; Wang, M. D.; et al. *Biophys. J.* **1997**, *72*, 1335; Chu, S. *Rev. Mod. Phys.* **1998**, *70*, 685.

(23) Rief, M.; Gautel, M.; Oesterhelt, F.; Fernandez, J. M.; Gaub, H. E. *Science* **1997**, *276*, 1109.

(24) Evans, E.; Ritchie, K. *Biophys. J.* **1997**, *72*, 1541.

(25) Wentrup, C. *Reactive molecules: the neutral reactive intermediates in organic chemistry*; Wiley: New York, 1984; p 88.

(26) Saitta, A. M.; Klein, M. L. *J. Am. Chem. Soc.* **1999**, *121*, 11827.

(27) Ashley, C. W. *The Ashley Book of Knots*; Doubleday: New York, 1993.

(28) Arai, Y.; et al. *Nature* **1999**, *399*, 446.